Manuscript

Click here to access/download;Manuscript;Cryogenic exposure on composite interface.docx

MECHANICAL PROPERTIES OF CARBON FIBER REINFORCED COMPOSITES EXPOSED TO CRYOGENIC CONDITIONS AND SPACE RADIATION VIA SIMULATION AND TESTING

Eric R. Messer[1], Siddhesh Chaudhari[1], Eric Benton[2], Enrique M. Jackson[3], Travis Alley[4], Matt Villarreal[4], Subhabrata Saha[5], Ranji Vaidyanathan[1]

[1]School of Materials Science and Engineering, Oklahoma State University, Tulsa, OK

[2]Department of Physics, Oklahoma State University, Stillwater, OK

[3]NASA Marshall Space Flight Center, Huntsville, AL

[4]Infinite Composites Inc., 10738 E 55th Pl, Tulsa, OK

[5]Manufacturing Demonstration Facility, Oak Ridge National Laboratory, Oak Ridge, TN

ABSTRACT

As NASA missions extend beyond low Earth orbit, increasing reliance is placed on carbon fiber reinforced polymer (CFRP) composites for spacecraft structures where mass efficiency, durability, and long-term reliability are critical. In service, these materials are subjected to a combination of ultraviolet radiation, vacuum, ionizing radiation, atomic oxygen, and extreme thermal excursions under sustained mechanical loading. Flight systems such as the Boeing Starliner and SpaceX Dragon employ external composite structures that will experience these environments for extended durations. Although prior spaceflight and ground studies have reported limited changes in bulk mechanical properties, the synergistic effects of these environments on composite microstructure, particularly at the fiber matrix interphase, remain insufficiently characterized and represent a potential qualification and reliability risk.

This study investigates the effects of short-term cryogenic exposure on a radiation shielding carbon epoxy composite, SC2020, as a ground-based analog for space relevant thermal extremes. The SC2020 material system has previously flown on the International Space Station under the Materials International Space Station Experiment (MISSE) program. Composite specimens were exposed to liquid nitrogen for 6 and 24 hours and evaluated using a multiscale characterization framework that combined ASTM D3039 tensile testing, Atomic Force Microscopy based interphase analysis, and helium gas permeability measurements. Tensile testing showed no statistically significant or permanent degradation in global strength or modulus following cryogenic exposure. In contrast, AFM measurements revealed reductions in interphase modulus, weakened adhesion, and increased nanoscale heterogeneity, indicating localized degradation mechanisms not captured by conventional bulk testing. Gas permeability measurements showed a progressive increase in helium diffusion with exposure duration, consistent with micro-void formation or partial interfacial debonding.

The results indicate that cryogenic exposure initiates degradation at the fiber matrix interphase while leaving global mechanical properties largely unchanged over short durations. These findings underscore the importance of multiscale diagnostics for identifying early-stage damage mechanisms that may influence long term performance and qualification margins for spaceflight composite structures. The data presented establish a cryogenic baseline for comparison with forthcoming MISSE flight exposure results and support ongoing NASA EPSCoR efforts aimed at improving composite qualification methodologies, risk assessment, and reliability prediction for space environments.

Keywords: Cryogenic exposure, CFRP composites, interphase degradation, AFM, tensile testing, permeability, DSC, composite reliability
Corresponding author: Dr. Ranji Vaidyanathan, vaidyan@okstate.edu

1. INTRODUCTION

Carbon fiber-reinforced polymer (CFRP) composites are a mainstay in aerospace structures due to their high strength-to-weight ratio, corrosion resistance, and design flexibility. Their use is particularly critical in deep space missions, where mass efficiency and thermal stability are paramount. However, the space environment imposes severe conditions, including ultraviolet (UV) radiation, vacuum, atomic oxygen, ionizing radiation, and extreme thermal cycling. These factors can synergistically degrade composite properties, particularly at the fiber–matrix interphase, a zone critical to load transfer and mechanical integrity.

Oklahoma State University has recently developed SC2020, a carbon/epoxy composite designed for enhanced radiation shielding, which was flown aboard the International Space Station (ISS) as part of the Materials International Space Station Experiment (MISSE-11) [1,2]. While previous studies have indicated minimal changes in bulk mechanical properties due to space exposure, nanoscale mechanisms of degradation, particularly at the interphase, remain poorly characterized. This lack of insight may mask early-stage damage that could eventually compromise performance under service loads.

To address this knowledge gap, the present study investigates the effects of cryogenic exposure on SC2020 composites as a ground-based analog for space thermal extremes. Specifically, we combine macro-scale tensile testing with nanoscale Atomic Force Microscopy (AFM) to assess changes in mechanical and interfacial properties following immersion in liquid nitrogen [2]. This multi-scale approach enabled identification of subtle degradation mechanisms that may not be captured through conventional mechanical testing alone. The outcomes are expected to support qualification methodologies for future space-bound composite structures.

2. EXPERIMENTATION

2.1 Composite Fabrication

The composite used in this study, referred to as SC2020, was fabricated using T800S-24K carbon fiber and a five-part cryogenic-tolerant epoxy resin system. The material was manufactured via filament winding on a 12-inch square aluminum mandrel. The winding pattern was designed to replicate conditions used in pressure vessel applications, ensuring uniform fiber distribution. Following winding, the laminates were vacuum bagged and cured according to a controlled thermal cycle. The cured plates were then demolded and machined into rectangular specimens for tensile testing and smaller squares for interphase characterization. Figure 1a is an image of the square mandrel and Figure 1b is filament-wound panel on square mandrel after cure.

(a) (b)

Figure 1. Image of the filament-wound panel on square mandrel prior to cure and cured sample

The mandrel was a custom-designed square structure made with an aluminum head and tail, acrylic side plates, and stainless-steel rods and bolts. The aluminum head and tail sections provided robust structural support, while the acrylic side plates offered a lightweight but sturdy form to maintain the geometry during the winding process. Stainless steel rods and bolts were used to ensure structural integrity under the applied winding tensions. These bolts threaded through the aluminum plates and into the heat sink threads placed inside the acrylic side plates, providing a secure attachment mechanism that allowed for minimal deformation during the winding and curing stages. To ensure the carbon fiber-reinforced polymer did not adhere to the mandrel during curing, Teflon tape was applied to the mandrel surface, which facilitated easy removal of the cured specimen. The mandrel's square geometry was chosen to facilitate uniform application of shrink tape during the curing phase.

2.2 Sample Preparation for Tensile Testing and AFM

From the cured composite panels, specimens were cut into ASTM D3039 Type I dimensions (25.4 mm × 250 mm) for tensile testing. Tabbed ends were added using G-10 fiberglass with high-strength adhesive to prevent grip-induced failure. For AFM characterization, 12.7 mm × 12.7 mm × 3 mm square sections were precision-polished using silicon carbide abrasive films followed by diamond paste down to 0.05 μm. These samples were embedded in epoxy mounts and cured under controlled pressure to prevent edge lift during polishing. The AFM is an asylum Infinity located at the Oklahoma State University main campus in Stillwater, Oklahoma. The Asylum software is used to analyze the data collected by the AFM. The methods of gathering data are – no contact, full contact, and tap method. The data was analyzed using a fast force method specific to this system software. The CFRP samples removed from the mandrel shown in Figure 1 were sectioned into multiple small pieces so that it can be installed into the AFM and analyzed. Figure 2a are the machined tensile specimens with bonded G-10 tabs (Figure 2b), while Figure 3 is AFM sample mount with polished composite cross-section.

(a) (b)

Figure 2. Tensile specimens cut and bonded to tabs for tensile testing

Multiple samples were prepared and analyzed from a single mandrel run. The asylum Infinity software calculates the gain and the spring constant of the cantilever beam holding the tip on the FM. This allows quick imaging of the sample and offers direct calibration by the machine.

The samples prepared for AFM were cut from one of the four plates using a CNC water jet into dimensions of 12.7mm × 12.7 mm. These samples were subsequently placed in a modified silicon ice cube tray and embedded in resin for curing, as shown in Figure 3. The resin-embedded tray (Figure 3) was then placed in a vacuum oven for curing at 47°C for 24 hours. Following the curing process, the samples were sanded sequentially using silicon carbide sandpaper ranging from 480-grit to 5000-grit, and subsequently polished with an alumina suspension.

Figure 3. Composite samples prepared for AFM analysis

AFM samples were scanned at a resolution of 64 × 64 data points within 10 μm × 10 μm windows. Modulus was computed from individual force–distance curves using the Derjaguin–Muller–Toporov (DMT) model. Adhesion maps were generated concurrently. Scans were centered at the fiber–matrix interphase, with particular attention to post-exposure changes. Figure 4 is a representative AFM scan area of an unexposed sample with fiber, matrix, and interphase regions.

Figure 4. Representative AFM scan area of an unexposed sample with fiber, matrix, and interphase regions

2.3 Tensile Testing

Tensile tests were conducted using an Instron 4505 universal testing machine with a 100 kN load cell. Testing was performed at a crosshead speed of 2 mm/min. Strain was measured using bonded strain gauges centered between the tabbed regions. Data acquisition and control were handled via Bluehill software. For each exposure duration (0, 6, and 24 hours), at least three replicates were tested to ensure statistical reliability.

2.4 Helium Gas Permeability Testing

Permeability measurements were conducted to evaluate changes in microstructural integrity due to cryogenic exposure. These tests were conducted by at Oak Ridge National Laboratory. A Labthink VAC-V2 gas permeability tester was used with helium as the permeant gas. Disk-shaped specimens 50 mm in diameter were cut from cryogenically conditioned composite plates and mounted in the diffusion cell with O-ring sealing.

The permeability coefficient (P) was calculated using the steady-state flow method:

$$P = (V \times d \times \Delta p) / (A \times t \times \Delta C)$$

Where:

- V = volume of downstream chamber (cm^3)
- d = thickness of the specimen (cm)
- Δp = pressure differential across membrane (cmHg)
- A = test area (cm^2)
- t = time (s)
- ΔC = concentration difference of permeant gas

Tests were conducted at 25°C and averaged over three specimens per condition. Measurements were repeated for unexposed, 6-hour, and 24-hour cryogenically exposed samples. The test equipment is shown in Figure 5a and 5b and the machined specimens used for permeability tests are shown in Figure 6.

(a) (b)

Figure 5. Gas permeability tester at Oak Ridge National Lab used for permeability tests

Figure 6. 25.4 mm (1") diameter samples prepared for permeability tests

3. RESULTS

3.1 Tensile Testing

The tensile test results indicated minimal changes in bulk mechanical properties following cryogenic exposure. Unexposed specimens exhibited an average tensile strength of 1.69 ± 0.11 GPa and an elastic modulus of 61.5 ± 5.4 GPa. After 6 hours of cryogenic conditioning, the average strength decreased to 1.50 ± 0.09 GPa, with a slightly increased modulus of 63.1 ± 8.6 GPa. Following 24 hours of exposure, values returned close to baseline, with 1.68 ± 0.07 GPa for strength and 60.9 ± 1.7 GPa for modulus.

These results confirm that the SC2020 composite maintains global mechanical integrity under short-term cryogenic exposure, consistent with prior findings for similar carbon/epoxy systems exposed to space environments [3,5,6]. However, the variance in modulus after 6 hours may indicate underlying interfacial or matrix cracking, which is not readily captured by macro-scale testing. Table 1 shows the strength and modulus data for unexposed, 6 hours and 24 hours exposure.

Table 1. Strength and modulus data for unexposed, 6 hours and 24 hours cryogenic exposure

Composite and Cryogenic Exposure	**Tensile strength (GPa)**	**Standard deviation (GPa)**	**Tensile modulus (GPa)**	**Standard deviation (GPa)**
Unexposed	1.69	0.11	61.54	5.40
Exposed for 6 hours	1.50	0.09	63.05	8.64
Exposed for 24 hours	1.68	0.07	60.92	1.70

Figure 7a, 7b and 7c shows the representative stress–strain curves for 0, 6, and 24-hour exposed samples respectively, and Figure 8 shows the summary bar chart of tensile strength and modulus for the SC2020 composite samples.

(a) (b) (c)

Figure 7 (a-c). Representative stress-strain curves for CFRP composites for unexposed, 6 hours and 24 hours cryogenic exposure.

3.2 AFM Interphase Characterization

Atomic Force Microscopy (AFM) revealed critical changes in the interphase modulus and adhesion following cryogenic exposure. Fast Force Mapping showed that unexposed samples maintained distinct modulus contrast between fiber, matrix, and interphase regions. The average interphase modulus was approximately 1.93 GPa in unexposed samples.

After 6 and 24 hours of liquid nitrogen exposure, this contrast diminished significantly. Interphase regions showed lower average modulus values and greater heterogeneity in local stiffness. Adhesion maps similarly showed reduced attraction forces in the interphase zone, suggesting micro-level degradation in matrix bonding.

This nanoscale softening of the interphase aligns with earlier findings by Babu et al. [4,5], who demonstrated that UV and thermal cycling could selectively degrade the interphase without altering bulk tensile properties. In this case, cryogenic exposure appears to initiate similar early-stage damage pathways, validating the role of AFM as a predictive diagnostic tool for composite reliability.

Figure 9 shows the adhesion map for the unexposed, exposure for 6 hours and 24 hours respectively.

Figure 8. Summary bar chart of tensile strength and modulus of SC 2020

(a) (b) (c)

Figure 9 (a-c). Adhesion maps for unexposed, 6-hour and 24-hour exposure respectively

Figure 9 and associated analysis reveal the detrimental effects of cryogenic exposure on the interfacial adhesion properties of CFRP, with the interphase being the most affected region. Even though the impact here is measured in terms of cryogenic exposure, extreme environments could be evaluated in terms of exposure to hydrogen (gaseous or cryogenic). It could be expected that the interphase will be the main affected area in the case of a polymer composite.

3.3 Gas Permeability

Figure 10 shows the gas transmission rate of helium gas through the composite specimens.

Gas permeability tests revealed increased helium diffusion rates in samples exposed to cryogenic conditions. The permeability coefficient increased by 15% after 6 hours and 28% after 24 hours, indicating a progressive increase in microstructural permeability. This behavior suggests the formation of micro-voids or interfacial debonding not visible under optical microscopy.

These results support the hypothesis that cryogenic cycling can weaken interfacial adhesion and compromise the gas barrier performance of CFRPs. Zhou and Lucas [12] reported similar trends in epoxy systems exposed to moisture and freeze–thaw cycles. The observed increase in helium permeability further confirms that the degradation pathway begins at the interphase and propagates outward.

Figure 10. Gas pressure or gas transmission rate versus time using helium gas

3.4 Discussion

Exposure of composites to extreme environments such as cryogenic temperatures introduces a complex set of degradation mechanisms that manifest differently across material scales. While bulk mechanical properties may remain relatively stable in short-term exposures, as shown in this study, localized changes at the fiber–matrix interphase reveal a more sensitive pathway to structural compromise. These observations are consistent with previous research demonstrating that matrix microcracking, interfacial debonding, and phase separation can occur in composite systems subjected to thermal extremes [5,12].

In cryogenic environments, the mismatch in coefficients of thermal expansion between the fiber and matrix can induce residual stresses, particularly at the interphase. Over time, these stresses may lead to micro-void formation, altered adhesion, and modulus loss, especially when the thermal shock is repeated or prolonged. The AFM results in this study provide a clear illustration of these effects: interphase modulus decreased, adhesion weakened, and local variability increased with exposure duration. These nanoscale signals are critical in developing early-warning metrics for composite degradation.

When compared with space-exposed composites, as reported in past MISSE and NASA Langley studies [8,10], similar degradation pathways are noted. However, space exposure also includes UV and radiation effects, which may further accelerate damage at the interphase. Thus, while cryogenic exposure does not fully replicate the space environment, it offers a reliable and controllable analog to study one of the key stressors affecting composite structural integrity.

The results presented in this work describe the response of the composite systems to controlled cryogenic exposure, which represents a key environmental stressor relevant to low Earth orbit service conditions. At the time the experimental program was completed, space exposure data were not yet available due to changes in the MISSE-22 flight manifest. According to program communications, complications associated with the Russian launchpad infrastructure resulted in an accelerated launch schedule and the consolidation of all MISSE-22 carriers onto a single SpaceX-34 mission rather than distribution across multiple launch opportunities. While all ground qualification and test activities are proceeding as planned, the revised launch date is currently scheduled for 13 May 2026.

Given this revised schedule, incorporation of space exposed samples into the present study would have required a delay of more than one year before meaningful experimental data could be generated. To avoid this delay and to ensure timely evaluation of material performance, the present work focused on cryogenic exposure and post exposure characterization as an initial step. Cryogenic temperatures are widely recognized as one of the dominant contributors to composite degradation in space environments, particularly with respect to matrix embrittlement, thermally induced residual stresses, interfacial damage, and stiffness changes, as documented in the prior literature cited in this paper. The results reported here therefore provide a technically relevant assessment of composite behavior under one of the most severe and repeatable components of the space environment.

The data generated in this study also establish a baseline for direct comparison with future space flight results. By isolating cryogenic effects under controlled laboratory conditions, the present work supports improved interpretation of degradation mechanisms once additional environmental factors such as radiation exposure, vacuum conditions, atomic oxygen, and thermal cycling are introduced. In this context, the current analysis is intended to complement, rather than replace, forthcoming space exposure results.

4. LIMITATIONS OF THE CURRENT WORK AND FUTURE WORK

The primary limitation of the present study is the absence of direct space exposed composite samples. While cryogenic exposure captures an important subset of the space environment, it does not reproduce the combined effects of vacuum, ionizing radiation, atomic oxygen, and repeated thermal cycling experienced in low Earth orbit. As a result, the conclusions drawn in this work are limited to degradation mechanisms dominated by low temperature effects and associated thermomechanical responses.

This limitation will be addressed through planned post flight characterization of composite specimens exposed during the MISSE-22 mission. Upon retrieval, the space exposed samples will be evaluated using the same experimental and analytical methods employed in the present study. This approach will enable direct comparison between cryogenically exposed and flight exposed materials and will allow separation of cryogenic dominated degradation from effects associated with radiation induced chemical changes, vacuum related mass loss, and surface driven damage mechanisms. The resulting data set is expected to strengthen degradation models and improve confidence in ground-based screening methods used for space qualified composite systems.

Future work will therefore focus on integrating space exposure results with the cryogenic baseline established here, with the objective of refining mechanistic understanding and improving prediction of long duration composite performance in space environments relevant to aerospace and defense applications.

5. CONCLUSIONS

This study evaluated the response of a carbon fiber reinforced epoxy composite (SC2020) to short term cryogenic exposure using a coordinated set of bulk, microscale, and nanoscale characterization techniques. The tensile test results demonstrate that short duration cryogenic conditioning up to 24 hours produces no statistically significant or permanent degradation in global tensile strength or elastic modulus. These findings confirm that the composite retains its overall load bearing capability under limited cryogenic exposure, consistent with prior observations for aerospace grade carbon epoxy systems.

In contrast to the relatively stable bulk mechanical response, nanoscale characterization revealed clear evidence of localized degradation within the fiber matrix interphase. Atomic Force Microscopy measurements showed reductions in interphase modulus, weakened adhesion, and increased spatial heterogeneity following cryogenic exposure. These changes indicate that the interphase is the most sensitive region of the composite to cryogenic stress, even when macro scale properties appear unaffected. The observed interphase softening and adhesion loss are consistent with thermally induced residual stresses arising from coefficient of thermal expansion mismatch between fiber and matrix.

Gas permeability measurements further corroborate this interphase driven degradation mechanism. The progressive increase in helium permeability with exposure duration suggests the formation of micro-voids or partial interfacial debonding that are not detectable through conventional optical or bulk mechanical testing. Together, the AFM and permeability results demonstrate that cryogenic exposure initiates damage at the interphase, which can compromise functional properties such as barrier performance prior to measurable loss in structural strength.

Taken collectively, these results highlight the importance of multi scale characterization for assessing composite reliability in extreme environments. While conventional tensile testing is effective for evaluating global performance, it is insufficient for detecting early-stage damage mechanisms that originate at the interphase. AFM based interphase analysis, when combined with functional measurements such as gas permeability, provides a sensitive and predictive framework for identifying degradation pathways before they manifest as macroscopic failure.

Although cryogenic exposure does not replicate the full space environment, it represents a dominant and controllable stressor relevant to low Earth orbit applications. The results presented here establish a baseline for comparison with forthcoming space flight data from MISSE-22 and will enable clearer separation of cryogenic effects from those associated with radiation, vacuum, atomic oxygen, and thermal cycling. From a materials engineering perspective, these findings inform composite selection, interphase design, and qualification strategies for aerospace structures, cryogenic fuel containment systems, and other applications requiring reliable polymer composite performance under extreme thermal conditions.

6. ACKNOWLEDGEMENTS

The authors acknowledge the financial support by NASA EPSCoR (Grant No. 80NSSC23M0211). The authors also wish to acknowledge support from Infinite Composites and the Manufacturing Demonstration Facility at the Oak Ridge National Lab.

7. REFERENCES

1. Oklahoma State University. (2017). Assessment of Radiation Shielding Properties of Novel and Baseline Materials External to ISS (NASA EPSCoR Grant No. 80NSSC17M0036). National Aeronautics and Space Administration.
2. Oklahoma State University. (2023). Effect of synergistic space effects on properties of novel polymer composite materials (PCM) (NASA EPSCoR Grant No. 80NSSC23M0211). National Aeronautics and Space Administration.
3. Juby, Ian D. "Effect of Space Radiation on Composite Material that Was Internal and External of the Pressurized Volume on the International Space Station (ISS)." MS Thesis diss., Oklahoma State University, 2022.
4. Babu, Libin Kaleeluvilayil. "The Use of AFM Indentation to Quantify Mechanical Properties of the Interphase Region in Fiber-reinforced Composites." PhD diss., Oklahoma State University, 2019.
5. Babu, Libin K., Kunal Mishra, and Raman P. Singh. "Near–fiber effects of UV irradiation on the fiber–matrix interphase: A combined experimental and numerical investigation." *Materials & Design* 157 (2018): 294-302.
6. Woo, Ricky SC, Honggang Zhu, Christopher KY Leung, and Jang-Kyo Kim. "Environmental degradation of epoxy-organoclay nanocomposites due to UV exposure: Part II residual mechanical properties." *Composites science and technology* 68, no. 9 (2008): 2149-2155.

7. Pastore, R., A. Delfini, M. Albano, A. Vricella, M. Marchetti, F. Santoni, and F. Piergentili. "Outgassing effect in polymeric composites exposed to space environment thermal-vacuum conditions." *Acta Astronautica* 170 (2020): 466-471.
8. De Groh, Kim K., and Bruce A. Banks. "The MISSE-9 Polymers and Composites Experiment Being Flown on the MISSE-Flight Facility." In *International Space Station Research and Development (ISSR&D) Conference 2017*, no. GRC-E-DAA-TN43550. 2017.
9. Rojdev, Kristina. "Long term lunar radiation degradation of potential lunar habitat composite materials." PhD diss., University of Southern California, 2012.
10. Gaier, James R., and Kim K. De Groh. "*Degradation of Intercalated Graphite Epoxy Composites Exposed to Low Earth Orbit*." Report No. E-19544. 2018.
11. Qian, D., et al. (2018). "Effects of thermal shock on the microstructures, mechanical and thermal properties of carbon fiber reinforced carbon matrix composites." *Composites Part B: Engineering*, 155, 1-9.
12. Zhou, J., & Lucas, J. P. (1999). "Hygrothermal effects of epoxy resin. Part I: the nature of water in epoxy." *Polymer*, 40(20), 5505–5512.
13. Sun, J., et al. (2022). "Nanoindentation of multifunctional smart composites." *Polymers*, 14(14), 2945.
14. Koerner, H., et al. (2018). NASA Langley Research in Fatigue of Composites. *NASA Technical Note*, DOT/FAA/TC-TN16/14.

Figures Click here to access/download;Manuscript;Figures for paper.docx

Figures for "MECHANICAL PROPERTIES OF CARBON FIBER REINFORCED COMPOSITES EXPOSED TO CRYOGENIC CONDITIONS AND SPACE RADIATION VIA SIMULATION AND TESTING"

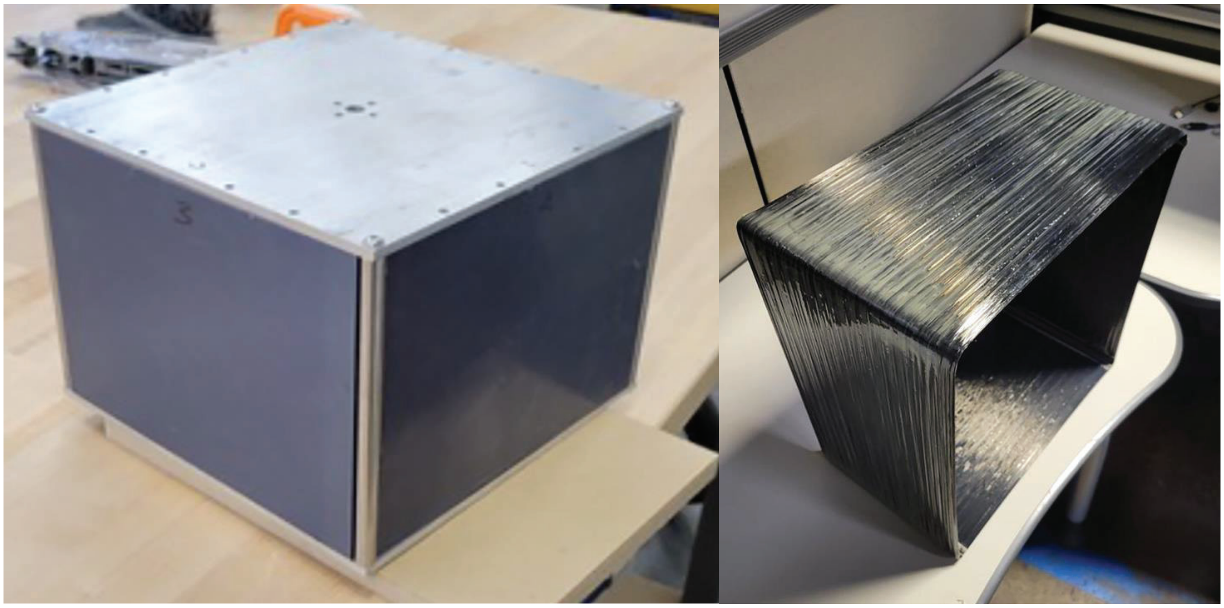

(a) (b)

Figure 1. Image of the filament-wound panel on square mandrel prior to cure and cured sample

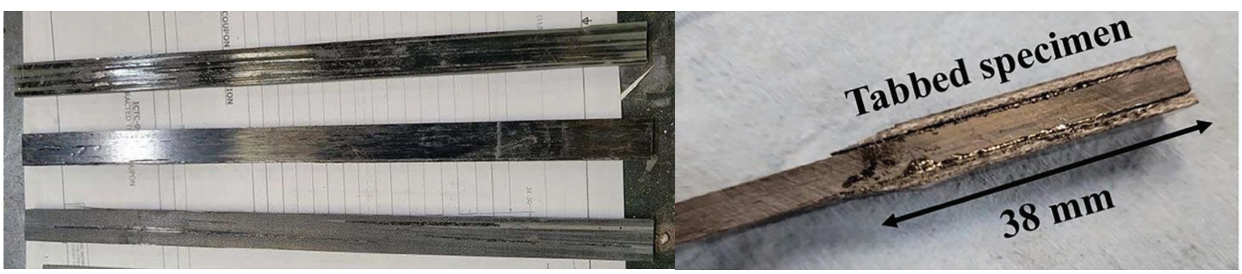

(a) (b)

Figure 2. Tensile specimens cut and bonded to tabs for tensile testing

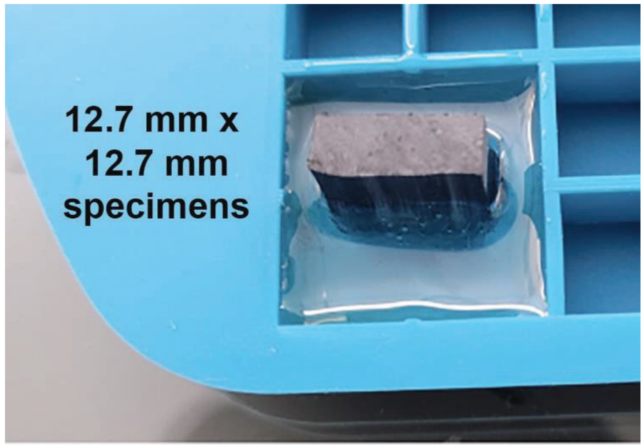

Figure 3. Composite samples prepared for AFM analysis

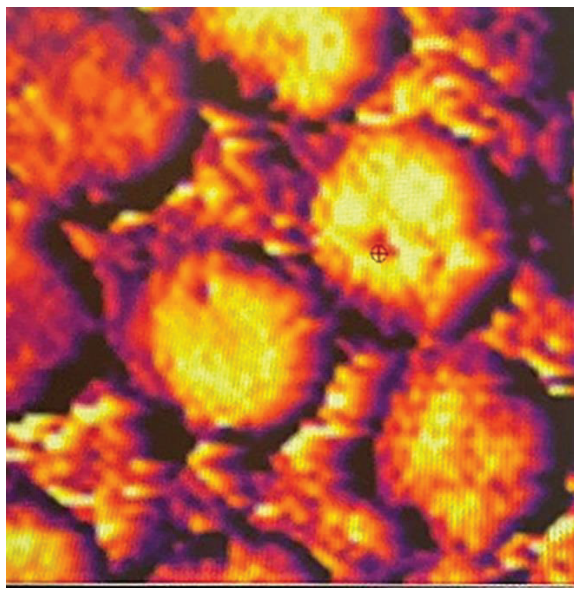

Figure 4. Representative AFM scan area of an unexposed sample with fiber, matrix, and interphase regions

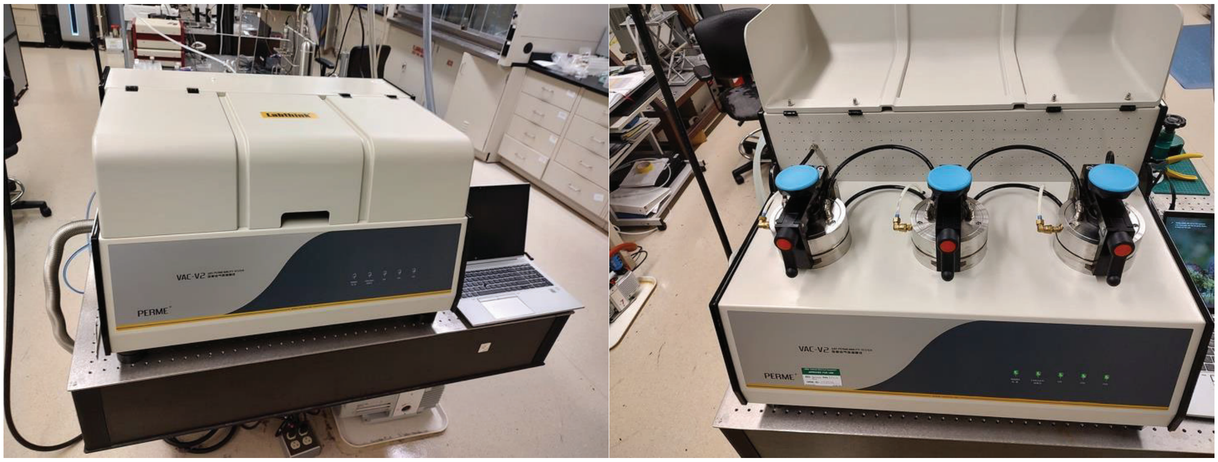

(a) (b)

Figure 5. Gas permeability tester at Oak Ridge National Lab used for permeability tests

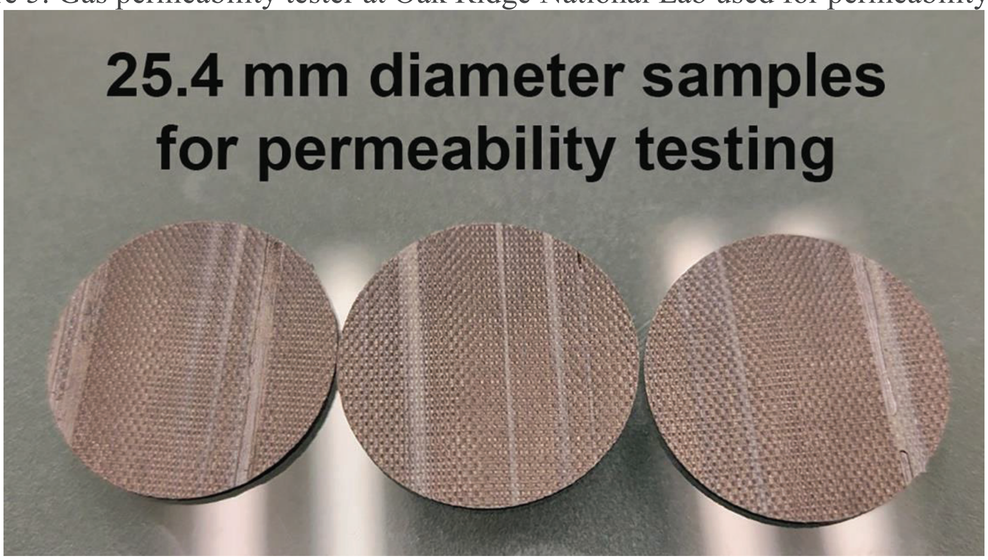

Figure 6. 25.4 mm (1”) diameter samples prepared for permeability tests

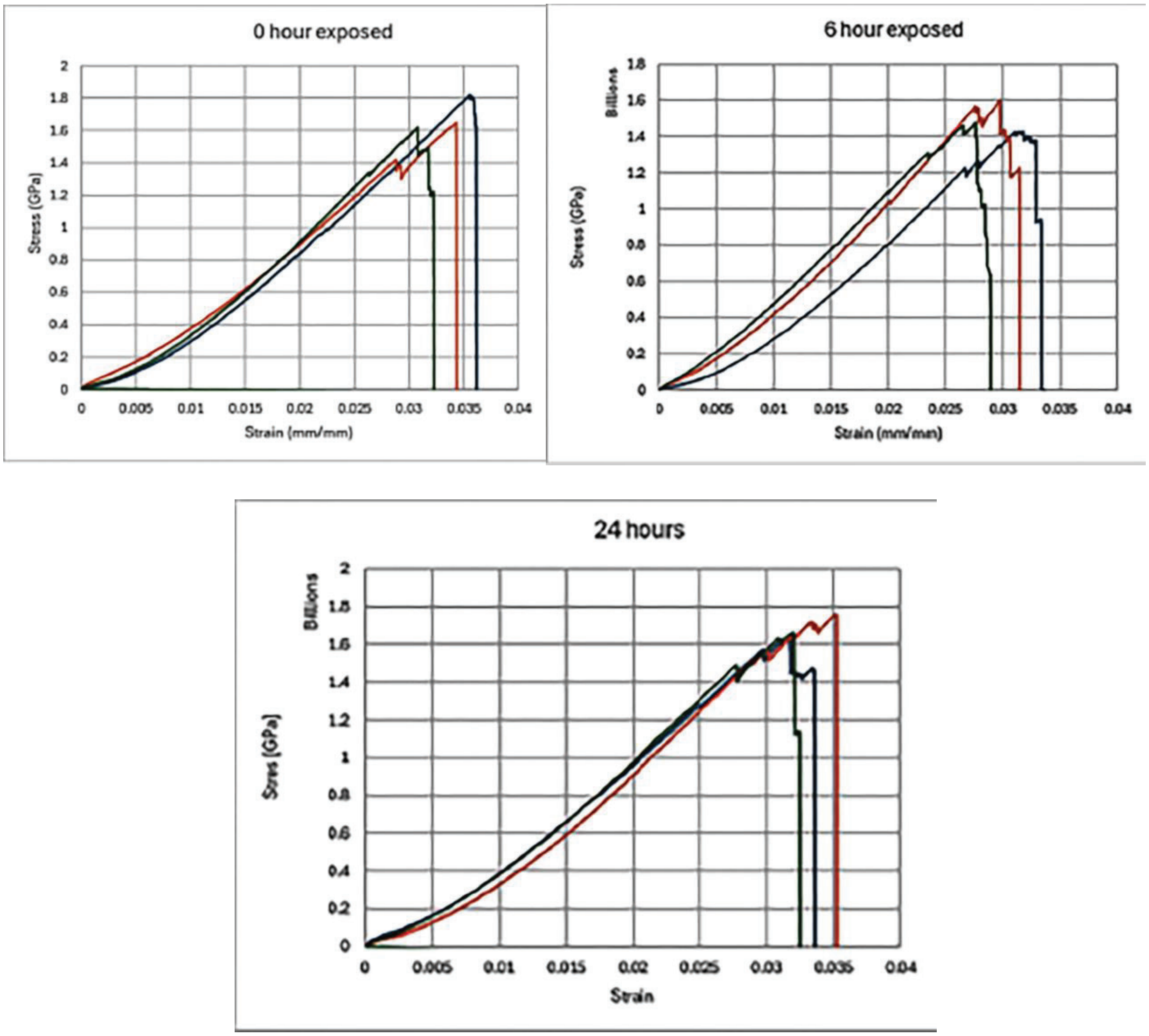

(a) (b) (c)

Figure 7 (a-c). Representative stress-strain curves for CFRP composites for unexposed, 6 hours and 24 hours cryogenic exposure.

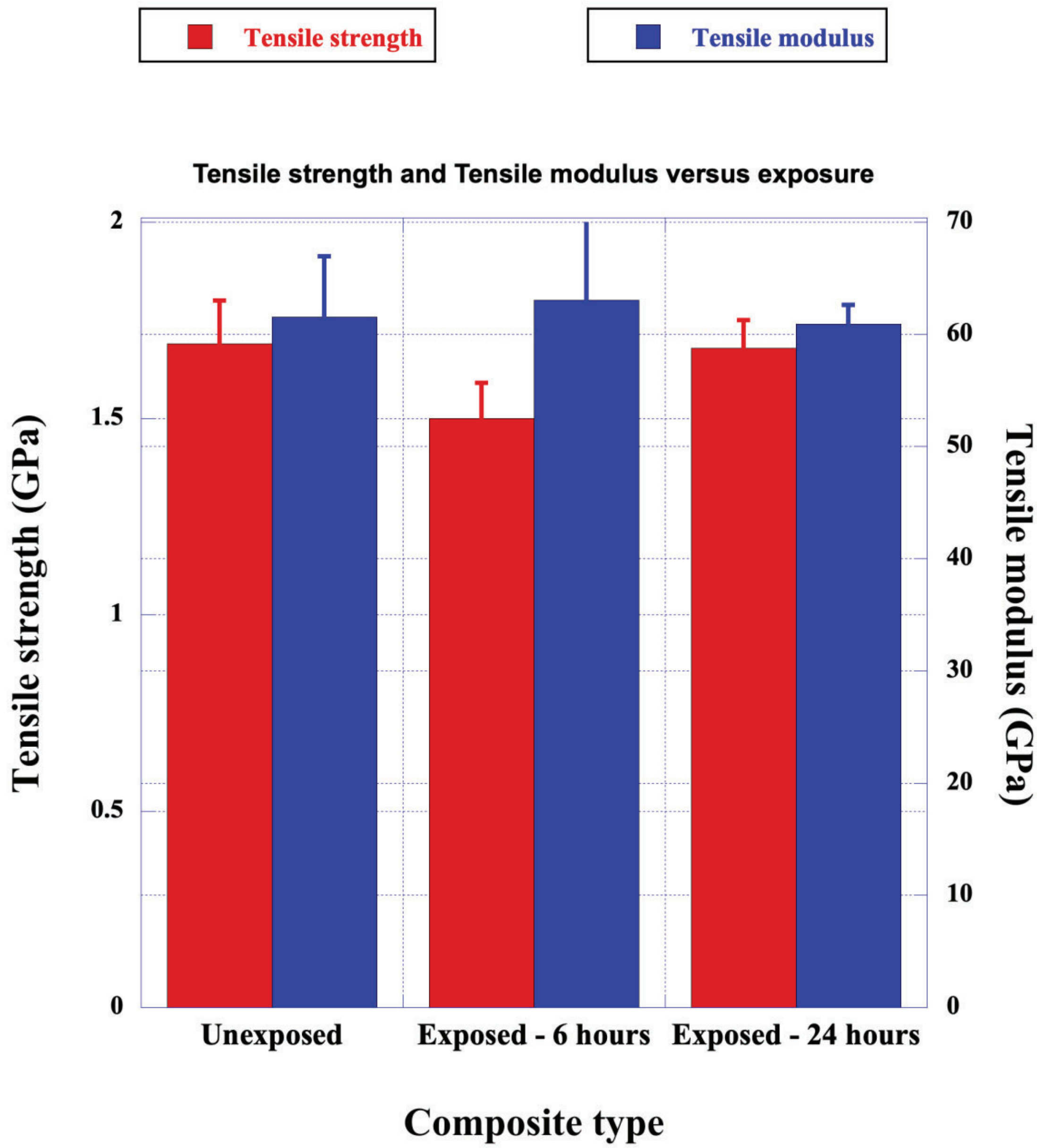

Figure 8. Summary bar chart of tensile strength and modulus of SC 2020

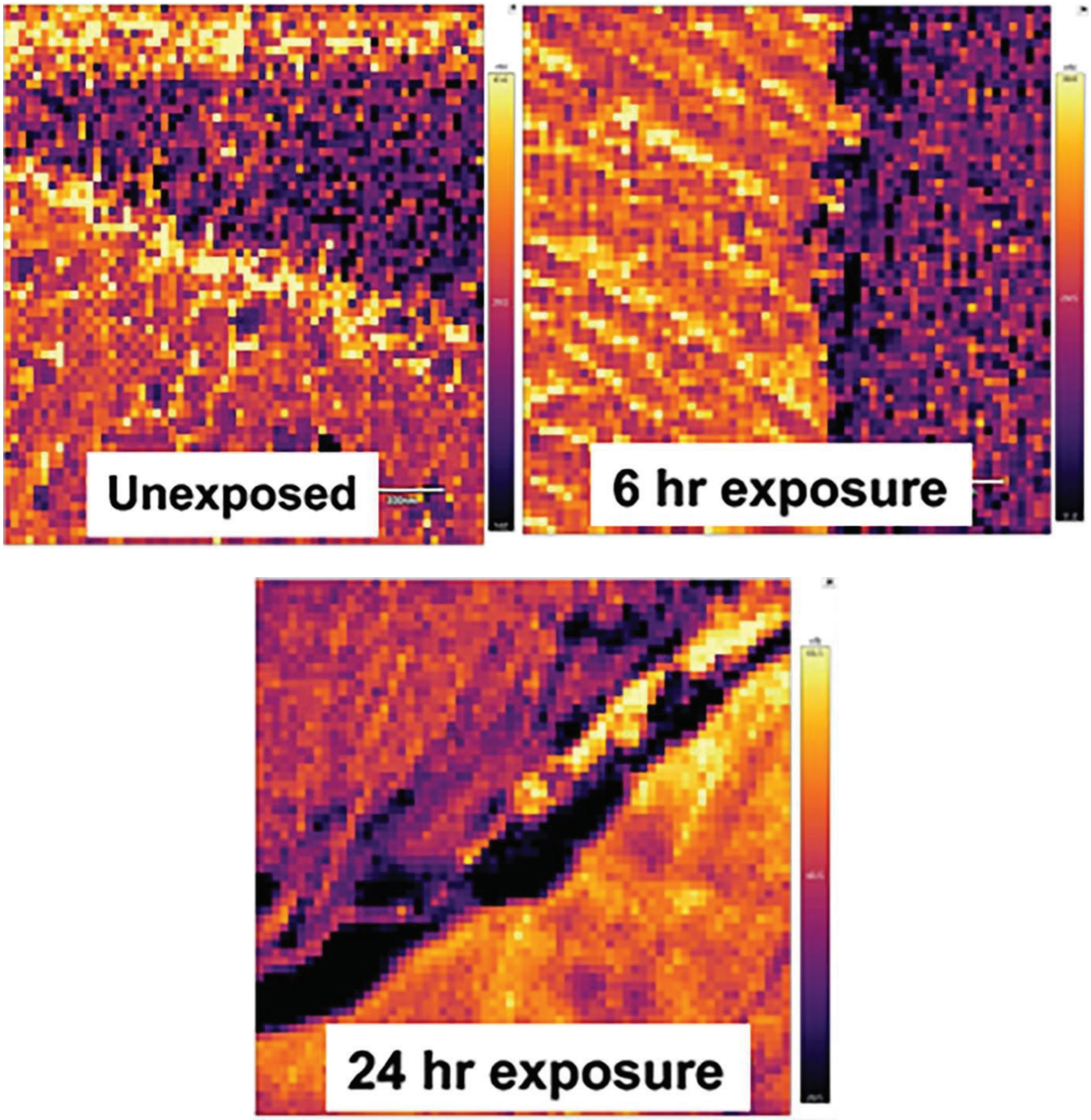

(a) (b) (c)

Figure 9 (a-c). Adhesion maps for unexposed, 6-hour and 24-hour exposure respectively

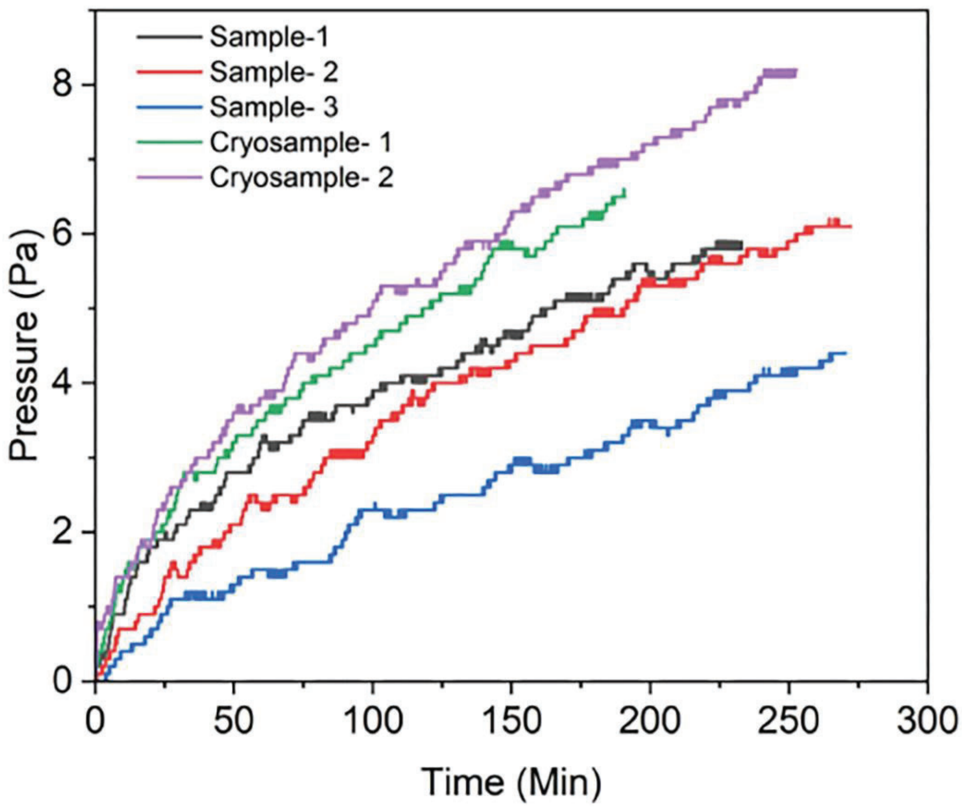

Figure 10. Gas pressure or gas transmission rate versus time using helium gas